LM-02K018
March 28, 2002

Hybrid Finite Element-Fast Spectral Domain Multilayer Boundary Integral Modeling of Doubly Periodic Structures

T.F. Eibert, J.L. Volakis, Y.E. Erdemli

Hybrid Finite Element–Fast Spectral Domain Multilayer Boundary Integral Modeling of Doubly Periodic Structures

Thomas F. Eibert, John L. Volakis and Yunus E. Erdemli
Radiation Laboratory, EECS Department
The University of Michigan, Ann Arbor, MI 48109-2122

Abstract

Hybrid finite element (FE) – boundary integral (BI) analysis of infinite periodic arrays is extended to include planar multilayered Green's functions. In this manner, a portion of the volumetric dielectric region can be modeled via the finite element method whereas uniform multilayered regions can be modeled using a multilayered Green's function. As such, thick uniform substrates can be modeled without loss of efficiency and accuracy. The multilayered Green's function is analytically computed in the spectral domain and the resulting BI matrix–vector products are evaluated via the fast spectral domain algorithm (FSDA). As a result, the computational cost of the matrix–vector products is kept at $O(N)$. Furthermore, the number of Floquet modes in the expansion are kept very few by placing the BI surfaces within the computational unit cell. Examples of frequency selective surface (FSS) arrays are analyzed with this method to demonstrate the accuracy and capability of the approach. One example involves complicated multilayered substrates above and below an inhomogeneous filter element and the other is an optical ring-slot array on a substrate several hundred wavelengths in thickness. Comparisons with measurements are included.

1 Introduction

Despite the availability of fast computational techniques for solving electromagnetics problems, the infinite array model is still an important approach for analysis and design of large finite arrays. A key aspect of the periodic array model is the use of periodic boundary conditions (PBCs) to reduce the computational domain down to a single unit cell, thus significantly speeding up analysis and reducing memory resources.

Early analyses on arrays and frequency selective surfaces concentrated on the application of Floquet's theorem to construct periodic Green's functions in the context of integral equation

(IE) formulations. Typically, the spectral domain (SD) of the Green's function is used [1] coupled with cascading for dealing with multilayer structures. The spectral domain formulation has also been extended to multilayered planar structures such as aperture coupled microstrip patches [2, 3]. More recently, the free periodic Green's functions have been incorporated into hybrid finite element (FE)–boundary integral (BI) methods [4, 5, 6, 7, 8, 9] for analysis of full three-dimensional (3D) structures (FSS and antennas) which may include inhomogeneous sections. In this context, the FE method is employed to model a unit cell representing the array and the BI provides for a rigorous mesh truncation at the upper and/or lower surfaces of the discretized unit cell.

Many array configurations can be analyzed by employing the appropriate half-space periodic Green's functions for the BI. However, modern array designs often require complex substrates and superstrate configurations. In the case of thick, possibly multilayered substrates/superstrates, it is not efficient to use the FE method to model the dielectric region. Instead, it is more appropriate to employ the multilayer Green's function in the context of the FE–BI method.

In this manner (see Fig. 1), the FE method is only used to model the inhomogeneous section of the domain which may involve metallizations or imperfect surfaces whereas the thick multilayer substrates/superstrates can be modeled using the multilayer spectral Green's functions. When compared with the standard implementations, the key difference in the proposed hybridization is the placement of the BI at the interface separating the multilayer region with the finite element domain. In previous FE–BI formulations, the BI had been placed at the interface of the FE domain with the free space region. The multilayer Green's function has been used in the context of the FE–BI in [10, 11] but not for periodic array applications. When dealing with periodic structures in the presence of multilayered layers, the SD form of the Green's function is particularly attractive. Of particular importance is the use of the SD representation of the multilayer Green's function in the recently introduced fast spectral domain algorithm (FSDA) [9] to attain $O(N)$ CPU and memory requirements. In this manner, very thick substrates can be modeled accurately even though they span several hundred wavelengths as is the case with millimeter wave and infrared filters.

Below, we begin by presenting the FE–BI formulation in a manner that incorporates the multilayered Green's function. This is followed by the FSDA implementation for carrying out

the matrix-vector products. The method is validated by comparing the results with measured data for an infrared FSS on a 670 wavelengths thick substrate.

2 Formulation

2.1 Basic Hybrid FE–BI Formulation

Since the basic hybrid FE–BI formulation for the treatment of infinite periodic array configurations can be found in many references such as [4, 5, 8], we only give the necessary equations to define notation and carry out the implementation of the multilayered Green's function. As usual, an $e^{j\omega t}$ time dependence is assumed and suppressed throughout. Also, the array is assumed to be generated by periodic repetition of the unit cell, as shown in Fig. 1. The periodicity is in the xy–plane defined by the lattice vectors $\boldsymbol{\rho}_a, \boldsymbol{\rho}_b$ via the shifting relation

$$\boldsymbol{\rho}_{mn} = m\,\boldsymbol{\rho}_a + n\,\boldsymbol{\rho}_b\,. \tag{1}$$

where m and n are integers. On invoking the periodicity conditions given in [8], electromagnetic analysis can be carried out by minimizing the functional

$$\begin{aligned} F(\boldsymbol{E}_{\rm ad}, \boldsymbol{E}) \;=\; & \iiint_V \left[\frac{1}{\mu_{\rm r}}(\nabla \times \boldsymbol{E}_{\rm ad})\cdot(\nabla\times\boldsymbol{E}) - k_0^2\,\varepsilon_{\rm r}\boldsymbol{E}_{\rm ad}\cdot\boldsymbol{E} + jk_0Z_0\,\boldsymbol{E}_{\rm ad}\cdot\boldsymbol{J}^{\rm int}\right] dv \\ & + jk_0Z_0 \iint_S \boldsymbol{E}_{\rm ad}\cdot(\boldsymbol{H}\times\hat{\boldsymbol{n}})\,ds \end{aligned} \tag{2}$$

for the volume V of the FE portion of the unit cell, shown in Fig. 1. Here, $\boldsymbol{E}$ is the usual electric field, $\boldsymbol{E}_{\rm ad}$ is the solution of the adjoint field problem, $\boldsymbol{J}^{\rm int}$ denotes an excitation current interior to the FE domain, S represents the bounding surface of the FE domain, $\hat{\boldsymbol{n}}$ is the unit surface normal directed out of the FE domain, $(\mu_{\rm r}, \varepsilon_{\rm r})$ are the relative dielectric constants of the medium, and k_0, Z_0 are the wave number and characteristic impedance of free space, respectively.

The quantity $\boldsymbol{H}\times\hat{\boldsymbol{n}}$ in the surface integral of (2) must be replaced by an expression in terms of $\boldsymbol{E}$ to obtain a well-posed formulation for solving $\boldsymbol{E}$. The BI method will be employed for this purpose. Further, since an arbitrary number of planar layers can be located outside the FE domain, the BI Green's function must be constructed to include the influence of these layers. Consequently, a dyadic Green's function $\bar{\boldsymbol{G}}_{\rm p}$ must be assumed and an appropriate BI

relation for the magnetic field intensity $\boldsymbol{H}$ applicable in the top and bottom BI surfaces S is given by

$$\boldsymbol{H}(\boldsymbol{r}) = \iint_S \bar{\boldsymbol{G}}_{\mathrm{p}}(\boldsymbol{r}, \boldsymbol{r}') \cdot (\boldsymbol{E}(\boldsymbol{r}') \times \hat{n})\, ds' + \boldsymbol{H}^{\mathrm{exc}}(\boldsymbol{r})\,. \tag{3}$$

By virtue of the infinite planar surface separating the FE and multilayer domain, we can follow the approach in [8, 9] and introduce equivalent magnetic currents $\mathbf{M}_S = \mathbf{E} \times \hat{n}$ above the FE surface. As such, $\mathbf{E}$ field continuity is maintained and this is the basis of (3).
The magnetic currents can radiate on a fictitious metallic surface, and the possible external excitation field $\boldsymbol{H}^{\mathrm{exc}}(\boldsymbol{r})$ must be computed in the presence of these metallic interfaces.

Substituting (3) in the FE functional (2) enforces continuity of the magnetic field across the FE domain interface and results in a well-posed weak formulation of the array problem. The FE and the BI discretization can next be performed as discussed in [8, 9] except that a multilayered Green's function given below must be used and consequently appropriate modifications to the FSDA algorithm are also required.

2.2 Multilayer Green's Function

In accordance with the FSDA formulation [9], we proceed to transform (3) into the spectral domain (indicated by the "~") expression

$$\boldsymbol{H}(\boldsymbol{r}) = \iint_{k_x k_y} \tilde{\bar{\boldsymbol{G}}}_{\mathrm{p}}(k_x, k_y) \cdot (\tilde{\boldsymbol{E}}(k_x, k_y) \times \hat{n})\, e^{-jk_x x} e^{-jk_y y}\, dk_x\, dk_y + \boldsymbol{H}^{\mathrm{exc}}(\boldsymbol{r})\,, \tag{4}$$

where $\tilde{\bar{\boldsymbol{G}}}_{\mathrm{p}}(k_x, k_y)$ denotes the spectral representation of the periodic Green's function, given by

$$\tilde{\bar{\boldsymbol{G}}}_{\mathrm{p}}(k_x, k_y) = \frac{1}{A} \sum_{p=-\infty}^{\infty} \sum_{q=-\infty}^{\infty} \tilde{\bar{\boldsymbol{G}}}(k_x, k_y)\, \delta(\boldsymbol{k}_t - \boldsymbol{k}_{tpq})\,, \tag{5}$$

where $\delta(k)$ represents the usual delta function. The constant $A = |\boldsymbol{\rho}_a \times \boldsymbol{\rho}_b|$ is the cross-sectional area of the unit cell's top/bottom bounding surfaces,

$$\boldsymbol{k}_t = k_x \hat{x} + k_y \hat{y} \tag{6}$$

and

$$\boldsymbol{k}_{tpq} = \boldsymbol{k}_{t00} + \frac{2\pi}{A} \left[p(\boldsymbol{\rho}_b \times \hat{z}) + q(\hat{z} \times \boldsymbol{\rho}_a) \right] \tag{7}$$

is the so-called reciprocal lattice vector. Also, $\tilde{\boldsymbol{E}}(k_x, k_y)$ is the Fourier transform of the electric field intensity on the top/bottom apertures of the unit cell's FE domain.

The notation $\tilde{\tilde{\boldsymbol{G}}}(k_x, k_y)$ denotes the non-periodic spectral domain multilayer Green's function that can be derived analytically for arbitrarily planar layered structures on top and below the FE domain (see Fig. 2). For the numerical implementation of the hybrid method, only the x- and y-components of the fields must be considered in the BI surface ($z = z' = 0$) and the corresponding Green's function elements can be computed using the homogeneous transmission line formalism discussed in [12]. The resulting components of the dyadic spectral Green's function are found to be

$$\tilde{G}_{xx}(k_x, k_y) = \frac{-k_x^2}{k_x^2 + k_y^2} Y_{ii}^{\mathrm{TE}}(k_x, k_y) - \frac{k_y^2}{k_x^2 + k_y^2} Y_{ii}^{\mathrm{TM}}(k_x, k_y)\,, \tag{8}$$

$$\tilde{G}_{yy}(k_x, k_y) = \tilde{G}_{xx}(k_x, k_y)\,, \tag{9}$$

$$\tilde{G}_{xy}(k_x, k_y) = \frac{-k_x k_y}{k_x^2 + k_y^2} Y_{ii}^{\mathrm{TE}}(k_x, k_y) + \frac{k_x k_y}{k_x^2 + k_y^2} Y_{ii}^{\mathrm{TM}}(k_y, k_y)\,, \tag{10}$$

$$\tilde{G}_{yx}(k_x, k_y) = \tilde{G}_{xy}(k_x, k_y)\,, \tag{11}$$

where the Y_{ii} are the piece-wise homogenous transmission line Green's functions for the line currents in section i with a unit voltage source excitation in the same section i as shown in Fig. 2. The superscripts TE and TM indicate transversal electric and transversal magnetic fields, respectively (for further details see [12, 13]). Once the individual Green's function components are evaluated and tabulated for the required wavenumbers $\boldsymbol{k}_{tpq}$, the spectral domain BI is evaluated in accordance with the fast spectral domain algorithm (FSDA) discussed in [9]. The multilayered structures above and below the FE unit cell can thus be considered without any additional computational cost (except for the initialization of the Green's functions).

3 Results

For practical array problems, far field patterns or array transmission and reflection coefficients are typically computed. Thus, plane wave excitations and the plane wave fields radiated from the BI currents must be computed in the presence of the multilayered structures on top and/or below the FE unit cell.

An excellent example illustrating the strength of the presented hybrid fast spectral domain multilayer FE–BI algorithm is the "artificial puck plate" frequency selective surface (FSS) depicted in Fig. 3, presented and analyzed in [5, 8, 9]. The structure consists of several dielectric

layers above and below a thick metallic plate penetrated by a dielectric-filled cylindrical hollow waveguide with circular metallic irises in its apertures. Moreover, the unit cell is skewed at an angle of 60°. When the BI surfaces are placed above the top layer and below the bottom layer (as done in [8, 9]), our unit cell FE mesh comprises 104769 volume and 2160 surface unknowns in each of the top and bottom BI surfaces. On applying the multilayer Green's function approach proposed in the present work, the FE mesh is reduced down to 18373 volume edges (about 5 times less). Further, we note that the BI surfaces are slightly shifted away from the thick metallic plate (i.e., away from the strongly diffracting edges) so that only a few Floquet modes are needed (9 Floquet modes in total, $-1 < p < 1$ and $-1 < q < 1$ in (5)). The transmission and reflection results obtained using this new hybrid method are compared with method of moments (MoM) data from [5] in Fig. 4. The curves show quite good agreement except for slight differences at higher frequencies (about 1 dB for the transmission coefficient), but these differences are the same as those already found with the standard hybrid FE–BI computations in [8, 9]. Nevertheless, a speed-up by a factor of 7 (over the standard FE–BI method) is observed when using the new hybrid FE–BI approach with the multilayer Green's function.

The second investigated array structure is an optical ring-slot FSS filter on a very thick substrate with a unit cell as shown in Fig. 5. The substrate thickness of $t = 670$ μm is up to several hundred wavelength in the frequency range of interest, and thus it is impossible to model the substrate by finite elements. An analytical multilayer Green's function is required to correctly model this substrate. Therefore, our new hybrid approach is appropriately suited to analyze this structure. Three FE layers of thickness 0.05 μm were placed above and below the gold metallization to keep the number of Floquet modes low for the simulation. The required computer time for one frequency point (using a total number of 9 Floquet modes) was on the order of 10 to 20 sec. depending on the number of iterations (Pentium II PC with a 400 MHz processor). The computed power transmission coefficient of the array at normal incidence are given in Figs. 6 and 7 as a function of frequency/wavelength of the incident wave. The narrowband results in Fig. 6 are highly oscillatory and certainly cannot be observed in practical configurations. Therefore, broadband (incoherent) results were obtained by applying a moving average scheme using a Gaussian filter having a 3 dB bandwidth of 0.35 THz. These results are shown in Fig. 7 and demonstrate good agreement with the measured data obtained

by Spector et al. [14].

4 Discussion and Conclusions

We presented a new hybrid finite element (FE)–boundary integral (BI) formulation that employs the multilayered Green's function in the BI for periodic array analysis. Such a formulation is very advantageous when the BI is evaluated with a recently introduced fast spectral domain algorithm (FSDA) since it reduces the computational cost of the iterative solver down to $O(N)$. In contrast to traditional FE–BI formulations, the proposed method allows the flexibility of modeling part of the inhomogeneous dielectric using the FE method whereas the multilayer region is accounted for in BI via the multilayer Green's function. The resulting periodic array analysis code is thus extremely flexible and can be easily adapted to efficiently analyze a great variety of array configurations that may reside on very thick substrates. Another feature of the formulation is that the BI can be shifted away from resonating elements or other material inhomogeneities to keep the number of required Floquet modes low, thus simplifying the evaluation of the multilayer Green's function.

References

[1] R. Mittra, C. H. Chan, T. Cwik, Techniques for Analyzing Frequency Selective Surfaces — A Review, *Proc. IEEE*, vol. 76, No. 12, pp. 1593–1615, Dec. 1988.

[2] R. Pous, D. M. Pozar, A Frequency-Selective Surface Using Aperture-Coupled Microstrip Patches, *IEEE Trans. AP*, vol. 39, No. 12, pp. 1763–1769, Dec. 1991.

[3] H. Aroudaki, V. Hansen, H.–P. Gemünd, E. Kreysa, Analysis of Low–Pass Filters Consisting of Multiple Stacked FSS's of Different Periodicities with Applications in the Submillimeter Radioastronomy, *IEEE Trans. AP*, vol. 43, No. 12, pp. 1486–1491, Dec. 1995.

[4] D. T. McGrath and V. P. Pyati, "Phased Array Antenna Analysis with the Hybrid Finite Element Method," *IEEE Trans. Antennas Propagat.*, vol. 42, no. 12, pp. 1625–1630, Dec. 1994.

[5] E. W. Lucas and T. W. Fontana, "A 3-D Hybrid Finite Element/Boundary Element Method for the Unified Radiation and Scattering Analysis of General Infinite Periodic Arrays," *IEEE Trans. Antennas Propagat.*, vol. 43, no. 2, pp. 145–153, Feb. 1995.

[6] D. T. McGrath and V. P. Pyati, "Periodic Structure Analysis Using a Hybrid Finite Element Method," *Radio Science*, vol. 31, no. 5, pp. 1173–1179, Sep/Oct. 1996.

[7] J. D'Angelo and I. Mayergoyz, "Phased Array Antenna Analysis," in *Finite Element Software for Microwave Engineering*, Edited by T. Itoh, G. Pelosi, and P. P. Silvester, John Wiley & Sons, Inc., 1996.

[8] T. F. Eibert, J. L. Volakis, D. R. Wilton, and D. R. Jackson, "Hybrid FE/BI Modeling of 3D Doubly Periodic Structures Utilizing Triangular Prismatic Elements and a MPIE Formulation Accelerated by the Ewald Transformation," *IEEE Trans. Antennas Propagat.*, vol. 47, no. 5, pp. 843–850, May 1999.

[9] T. F. Eibert and J. L. Volakis, "Fast Spectral Domain Algorithm for Hybrid Finite Element/Boundary Integral Modeling of Doubly Periodic Structures," *IEE Proceedings Microwaves, Antennas and Propagation*, vol. 147, no. 5, pp. 329–334, Oct. 2000.

[10] T. F. Eibert and V. Hansen, "3D FEM/BEM–Hybrid Approach for Planar Layered Media," *Electromagnetics*, vol. 16, no. 3, pp. 253–272, May–June 1996.

[11] T. F. Eibert and V. Hansen, "3D FEM/BEM–Hybrid Approach Based on a General Formulation of Huygens' Principle for Planar Layered Media," *IEEE Transactions on Microwave Theory and Techniques*, vol. 45, no. 7, pp. 1105–1112, July 1997.

[12] L.B. Felsen, N. Marcuvitz, *Radiation and Scattering of Waves,* IEEE Press Series on Electromagnetic Waves, Piscataway, 1994.

[13] K. A. Michalski, D. Zheng, "Electromagnetic Scattering and Radiation by Surfaces of Arbitrary Shape in Layered Media, Part I: Theory," *IEEE Trans. Antennas Propagat.*, vol. 38, no. 3, pp. 335–344, Mar. 1990.

[14] S. J. Spector, D. K. Astolfi, S. P. Doran, T. M. Lyszczarz and J. E. Raynolds, "Infrared Frequency Selective Surfaces Fabricated Using Optical Lithography and Phase Shift Masks," *J. Vac. Sci. Technol. B*, vol. 19, no. 6, pp. 2757–2760.

Figure Captions

Figure 1: Array unit cell with indication of BI and periodic boundary condition (PBC) surfaces.

Figure 2: Unit cell configuration for the derivation of the multilayer Green's function. The parameters (ϵ_i, μ_i) refer to the dielectric constants in each layer.

Figure 3: Unit cell of the "artificial puck plate" FSS as presented in [5, 8, 9].

Figure 4: Reflection and transmission curves of the "artificial puck plate" FSS for TE–incidence ($\vartheta = 0^0, \varphi = 0^0$) as compared with the method of moments results given in [5].

Figure 5: Unit cell of an optical ring-slot filter, $t = 670$ μm, $w = 118$ nm (black surface on top of silicon refers to gold metallization).

Figure 6: Power percentage transmittance of the ring-slot array in Fig. 5 for normal incidence (narrow band, lossfree).

Figure 7: Broadband power percentage transmittance of the ring-slot array in Fig. 6 for normal incidence as compared with measured data. The broadband simulation results were obtained by applying moving-average of the narrow band data using a Gaussian filter curve having a 3 dB bandwidth of 0.35 THz. The term $\tan\delta$ in the figure refers to the loss tangent.

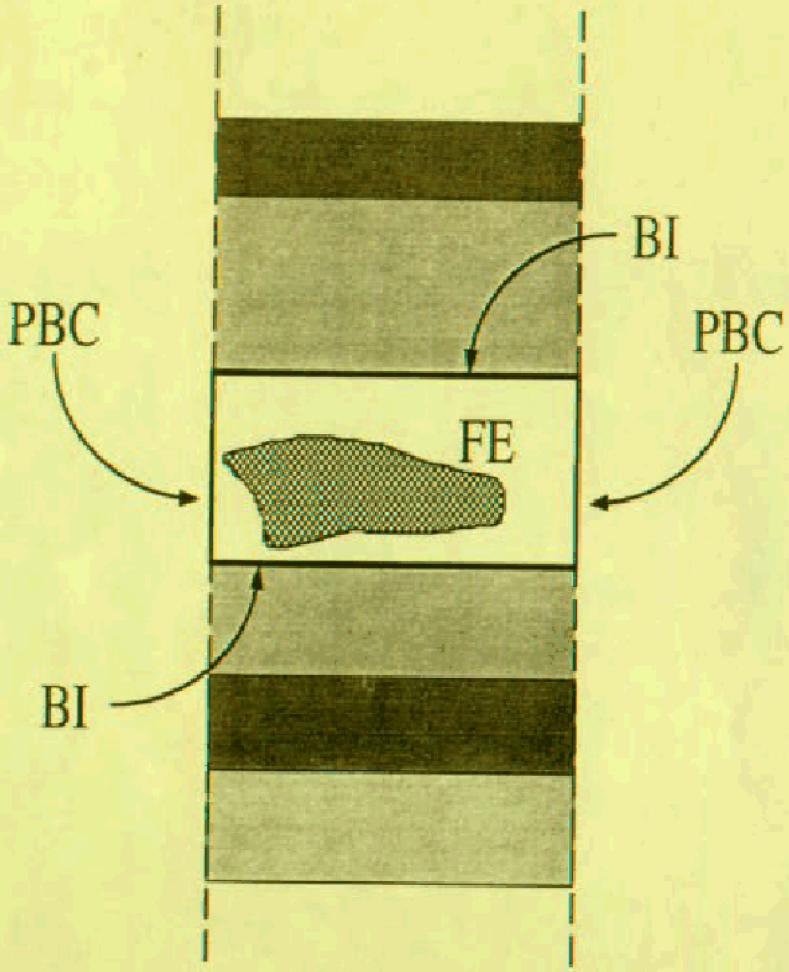

Figure 1:

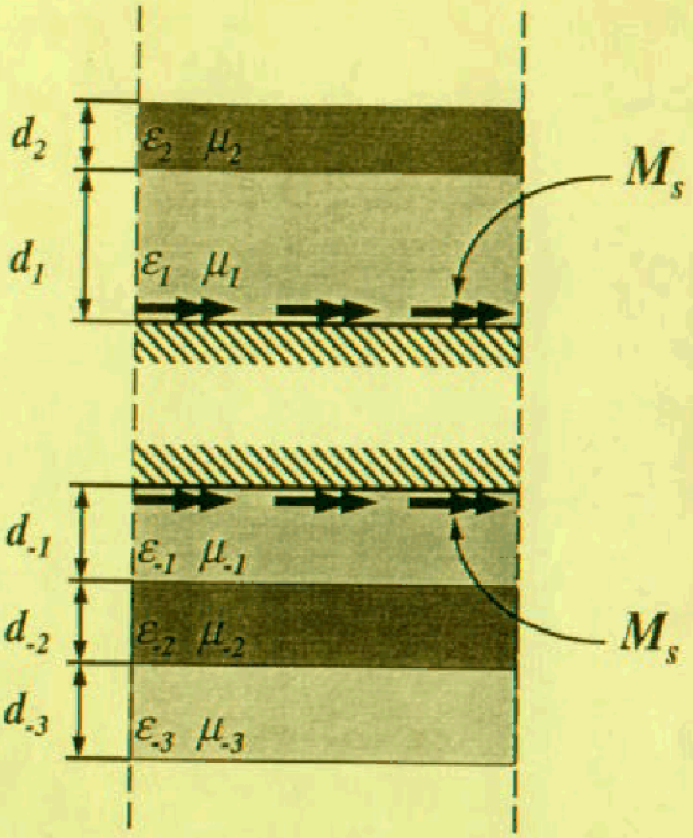
d_2
ε_2 μ_2
M_s
d_1
ε_1 μ_1
d_{-1}
ε_{-1} μ_{-1}
d_{-2}
ε_{-2} μ_{-2}
M_s
d_{-3}
ε_{-3} μ_{-3}

Figure 2:

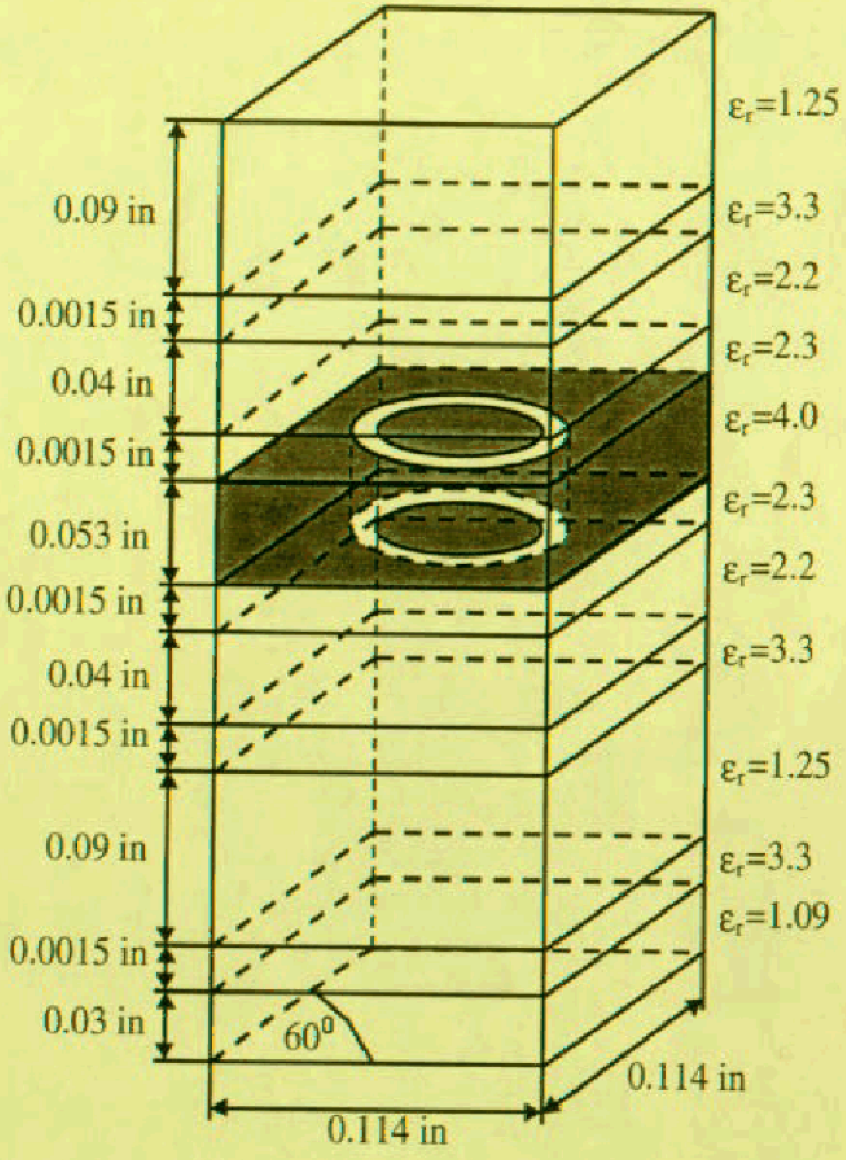

Figure 3: Unit cell of "artificial puck plate" FSS as presented in [5, 8, 9].

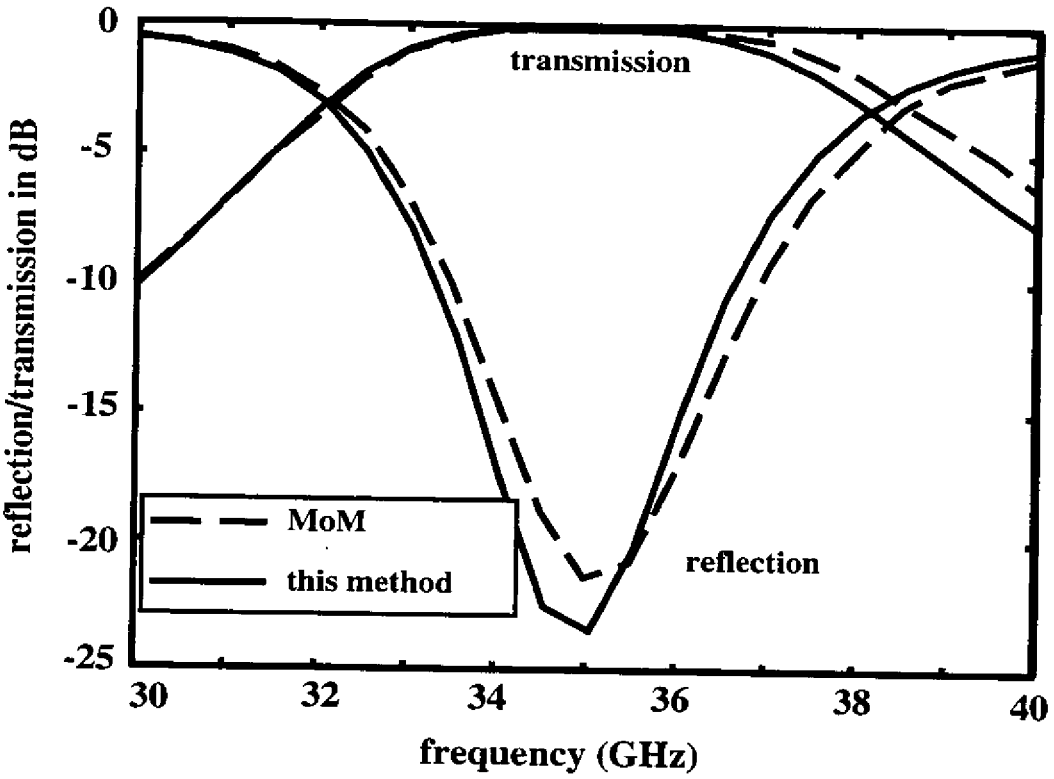
0
-5
-10
-15
-20
-25
reflection/transmission in dB
transmission
reflection
MoM
this method
30
32
34
36
38
40
frequency (GHz)

Figure 4:

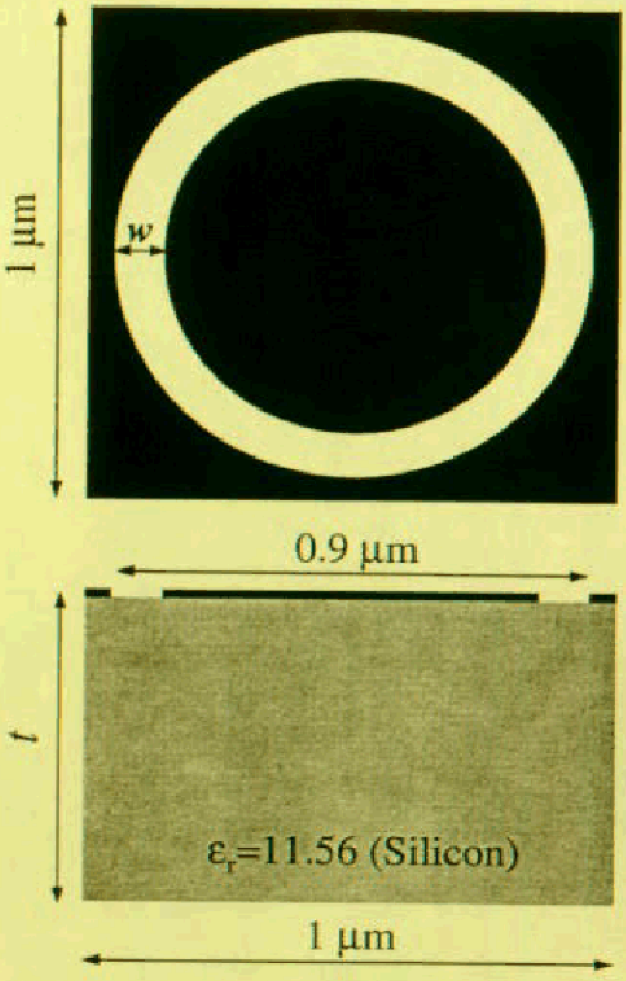

Figure 5:

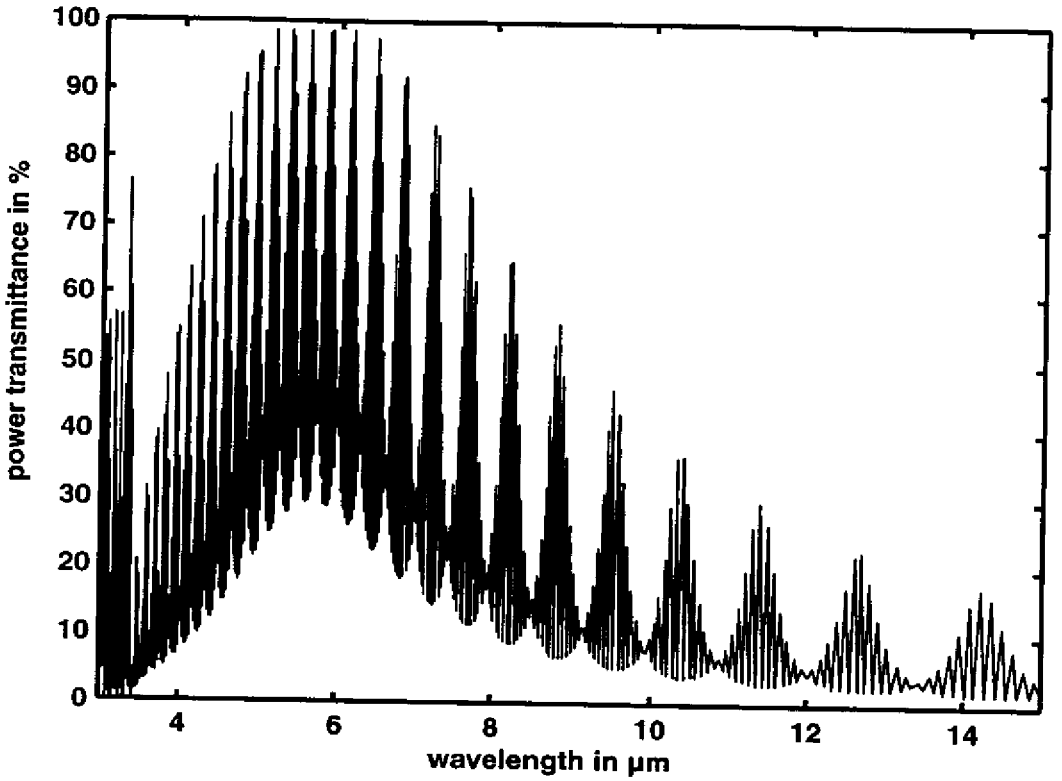
power transmittance in %
100
90
80
70
60
50
40
30
20
10
0
4
6
8
10
12
14
wavelength in µm

Figure 6:

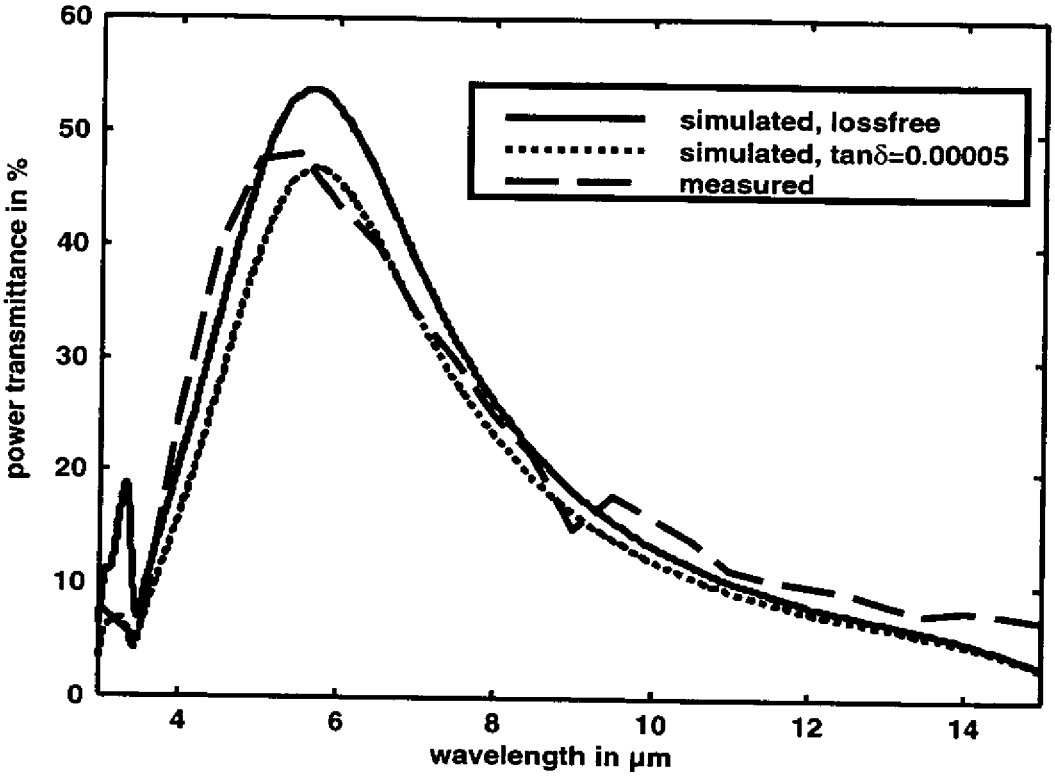
simulated, lossfree
simulated, tanδ=0.00005
measured
power transmittance in %
wavelength in µm
0
10
20
30
40
50
60
4
6
8
10
12
14

Figure 7: